Quadrupole interactions of ^{19}F implanted in germanium and gallium arsenide

D. Surono,* F-J. Hambsch, and P. W. Martin*

Commission of the European Communities Joint Research Centre, Institute for Reference Materials and Measurements, Retieseweg, 2440 Geel, Belgium

(Received 16 May 1995)

Time-differential perturbed angular distribution measurements on the 197-keV isomeric state in ^{19}F were performed using the ^{19}F$(p,p')^{19}$F* reaction to implant ^{19}F* into hosts of Ge and GaAs. In Ge two quadrupole frequencies were detected, with ν_{Q1}=27.5 (3) MHz and ν_{Q2}=33.0 (4) MHz, while in GaAs only a single interaction was observed, with ν_Q=27.7 (5) MHz. In all cases the asymmetry parameter η was close to or equal to zero. The results were compared with Hartree-Fock (HF) and density functional theory (DFT) calculations. In the case of germanium ν_{Q1} and ν_{Q2} are tentatively ascribed to antibonding and bond-centered sites, respectively. In the antibonding configuration the fluorine is situated at 1.88 Å along a ⟨111⟩ direction from a germanium atom. For F at the bond-centered site the Ge-Ge bond length was found to increase by about 1 Å from its normal lattice value. In gallium arsenide the single frequency ν_Q is consistent with calculations for F at an intrabond site with the fluorine situated at 1.37 Å from the Ga and 2.40 Å from the As atom. In all cases the DFT predictions are in better agreement with experiment than those of HF.

I. INTRODUCTION

In recent years the study of semiconductor materials using nuclear techniques has witnessed a rapid growth.[1] In particular, the techniques of time-differential perturbed angular correlations or distributions (TDPAD) of γ rays have been extensively employed.

The improvement of device characteristics obtained by the addition of fluorine in the semiconductor fabrication process has stimulated many investigations into the role played by fluorine in device operation.[2–10] Nevertheless, detailed information regarding the residence sites of F in semiconductors is still lacking. In this paper we report the results of TDPAD investigations following the implantation of ^{19}F in germanium and gallium arsenide. In a previous study of ^{19}F in Ge,[11] Bonde Nielsen *et al.* emphasized the need for quantitative calculations in order to establish the nature of the sites occupied by fluorine. We have performed such calculations here, using both Hartree-Fock (HF) and density functional theory (DFT) formalisms. To our knowledge, no quadrupole interaction studies have previously been reported for ^{19}F implantation in GaAs using the TDPAD technique.

II. EXPERIMENTAL DETAILS

The 7-MeV Van de Graaff at IRMM was operated in pulsed mode to provide 2.02-MeV incident protons with a beam burst width of 2 ns and repetition period of 1600 ns. The proton beam was directed to impinge on targets of 0.5-mm-thick crystalline wafers of ⟨111⟩ germanium and gallium arsenide coated with a 30 μg/cm^2 layer of CaF_2. The samples were oriented so that the ⟨111⟩ axis perpendicular to the sample surface lay in the detector plane at 45° to the incident beam. Recoiling ^{19}F nuclei in the isomeric state (J^π=5/2$^+$, $T_{1/2}$=88.5 ns) at 197-keV excitation energy were produced via the ^{19}F$(p,p')^{19}$F* reaction and implanted into the samples with preferential alignment perpendicular to the beam direction. During the isomeric state lifetime the quadrupole moment Q of the nucleus interacts with the local electric field gradient (efg), giving rise to a perturbed angular distribution for the deexcitation 197-keV γ rays.

Details of the apparatus and TDPAD measurements have been reported previously.[12] Detectors at 0° and 90° to the beam direction recorded the delayed time spectra of the γ rays to give the experimental ratio

$$R(t) = \frac{W(0°,t) - W(90°,t)}{0.5W(0°,t) + W(90°,t)},$$

where $W(\theta,t)$ are the counts at angle θ following background subtraction and normalization using the yield of the isotropic γ-ray line at 110 keV from ^{19}F.

III. ANALYSIS

The $R(t)$ data and associated Fourier power transforms for both Ge and GaAs samples are shown in Figs. 1–3. In the analysis of the data possible static quadrupole interactions were identified from the frequencies ν_{ij} observed in the Fourier spectra, where j designates one of the three components of interaction i. Owing to exponential damping of the Fourier amplitudes arising from the finite widths in the time resolution and efg interaction [see Eq. (1) below], the highest frequency component ν_{i3} is not always observable. Nevertheless the ratio ν_{i2}/ν_{i1} is sufficient to determine the quadrupole frequency $\nu_Q = eQV_{zz}/h$ and asymmetry parameter $\eta = (V_{xx} - V_{yy})/V_{zz}$ for each interaction.[13] For

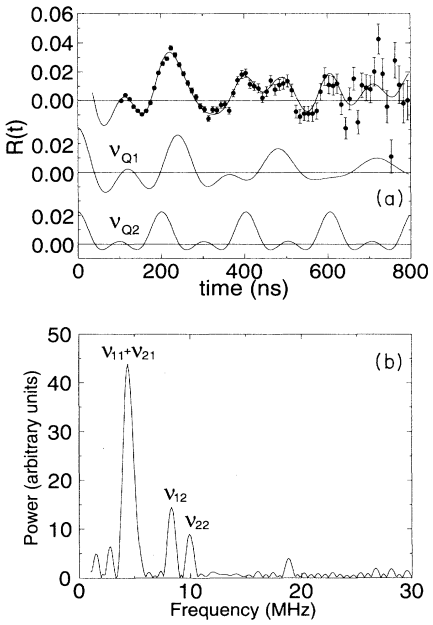

FIG. 1. (a) $R(t)$ data for ^{19}F implantation in Ge. The solid lines are fits to the data using the two interactions ν_{Q1} and ν_{Q2}. (b) The Fourier power transform of the $R(t)$ data for ^{19}F implantation in Ge.

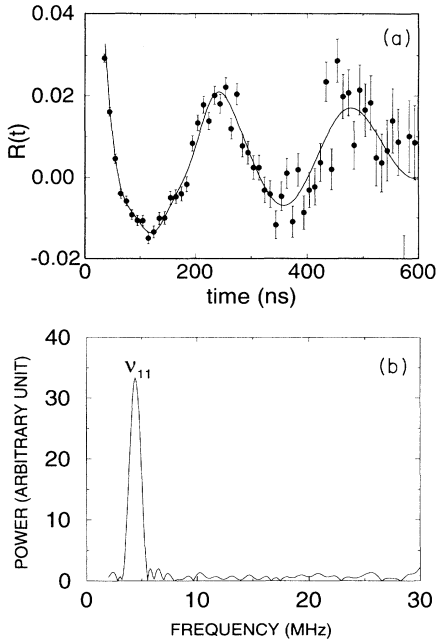

FIG. 3. (a) The $R(t)$ data of Fig. 2 with the exponential background subtracted. (b) The Fourier power transform of the $R(t)$ data for ^{19}F implantation in GaAs.

the Ge data fits to $R(t)$ were generated using as initial estimates the values of $\omega_0=3\pi\nu_Q/10$ and η derived from the Fourier spectra, with perturbation factor[14,15]

$$G_{k_1k_2}^{N_1N_2}(t)=\sum_{p=0}^{3}S_{k_1k_2p}^{N_1N_2}\exp[-\tfrac{1}{2}(g_p\omega_0\sigma)^2]\times\exp[-\tfrac{1}{2}(g_p\omega_0\delta t)^2]\cos(g_p\omega_0 t), \quad (1)$$

where σ and δ are Gaussian widths accounting for the finite resolving time and spread in the efg interaction, respectively, and the intraband frequencies are $\omega_p(\eta)=g_p(\eta)\omega_0$. For the case of GaAs, where ν_{12} was heavily suppressed [see Fig. 3(b)], the value of η was determined solely from the fit. In this instance, in order to ensure that a global minimum would be found for χ^2 in the parameter space, a Monte Carlo procedure was employed in the fitting routine to generate random starting values for η. The fits are shown as solid lines on the $R(t)$ spectra.

For comparison with theoretical calculations of the efg, the quantities of interest derived from the fits were $|V_{zz}|$, the principal component of the efg, and the asymmetry parameter, η.

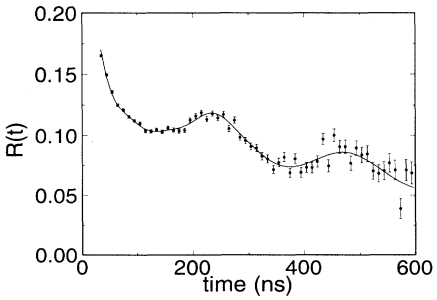

FIG. 2. The $R(t)$ spectrum for ^{19}F implantation in GaAs. The solid line is a fit to the data.

IV. THE EFG CALCULATIONS

A cluster model was used to calculate the efg at the site of ^{19}F in host matrices of Ge and GaAs. Using the GAUSSIAN 92 (G-92) computer code,[16] both HF and DFT formalisms were employed to calculate V_{zz} and η for the ^{19}F probe in specific configurations, with dangling bonds terminated by H atoms.[17] The atomic basis sets used were STO-3G*, i.e., Slater-type orbitals approximated by a sum of three Gaussians, where the asterisk indicates that d functions have been added to the heavy atoms.

The DFT calculations incorporated the local-spin-density exchange functional of Becke,[18] which includes corrections involving the gradient of the density, together with the correlation functional of Lee, Yang, and Parr,[19] which contains both local and nonlocal terms.

Since the calculations were extremely lengthy and costly in terms of CPU time, we restricted them to configurations for which G-92 predicted $\eta=0$, as indicated by the experimental results (see Table I).

TABLE I. Results of the fit to $R(t)$ for ^{19}F implantation in Ge.

Fraction (%)	Frequency (MHz)	η	δ (%)
58(3)	$\nu_{Q1} = 27.5(3)$	0.09(8)	6(1)
42(2)	$\nu_{Q2} = 33.0(4)$	0.00(8)	0(1)

V. RESULTS AND DISCUSSION

A. Implantation of ^{19}F in Ge

Table I summarizes the results of the fit to $R(t)$ for ^{19}F implantation in Ge. Two static quadrupole interactions with η equal to or close to zero were observed with frequencies ν_{Q1}=27.5(3) MHz and ν_{Q2}=33.0(4) MHz, in good agreement with the values of 27.3(4) and 33.4(4) MHz reported by Bonde Nielsen *et al.*[11] However, for the case of the 33-MHz interaction these authors refer the symmetry to a major principal axis with high index, or associate it possibly with a polycrystalline region of low symmetry. Taking Q=0.072(4) b as the quadrupole moment for the 197-keV level of ^{19}F,[20] frequencies ν_{Q1} and ν_{Q2} correspond to field gradients $|V_{zz}| = 1.58(9) \times 10^{22}$ V/m^2 and $1.90(11)\times10^{22}$ V/m^2, respectively. The contributions from each interaction are shown in Fig. 1(a).

Following the good agreement obtained with experiment for recent cluster model calculations at ^{19}F in silicon, and based on the strong similarity of the data from Si and Ge structures,[11,21,22] the efg calculations were performed for F situated at sites along ⟨111⟩ directions in the Ge lattice. Figures 4 and 5 illustrate the cluster configurations for ^{19}F at a bond-centered (BC) and an antibonding (AB) site, respectively, while Fig. 6 shows a schematic representation of the sites in the {110} plane of the diamond lattice structure. All the calculations were made for clusters with neutral charge. The results of the calculations for both BC and AB sites are shown in Table II, together with the charge q_F on the fluorine atom obtained from the Mulliken charge distribution.

Dangling bonds on the peripheral Ge atoms of Fig. 4 were completed with H atoms, resulting in a 27-atom cluster, FGe_8H_{18}. With F centrally located between two Ge atoms, the bond length d was allowed to vary until the total energy was minimized, resulting in an expansion from the lattice value of 2.4465–3.4305 Å.

In the antibonding case the cluster considered was $FGe_{10}H_{15}$, with the fluorine atom situated along the ⟨111⟩ antibonding direction at a distance λ from a germanium atom. The length λ was treated as a free parameter in the energy minimization, resulting in a best fit value for λ of 1.8796 Å.

As can be seen from Table II, both HF and DFT formalisms generate $|V_{zz}|$ values that are systematically higher than those obtained from experiment. It may be unrealistic to expect closer agreement with the measured values since only the minimal basis set STO-3G is available for fourth period elements in G-92. While the DFT values of $|V_{zz}^{AB}|$=1.996×10^{22} V/m^2 and $|V_{zz}^{BC}|$=2.638×10^{22} V/m^2 are closer to the experimental results, both formalisms show a systematic trend, predicting $|V_{zz}|$ to be lower at the antibonding site. Referring to the DFT predictions, the calculations indicate that the efg at the antibonding site is of the order of 20% lower than that at the bond-center position, reflecting the same trend in the experimental data. Given the comparable difference in the measured values for ν_{Q1} and ν_{Q2}, and following the results of similar calculations for ^{19}F in

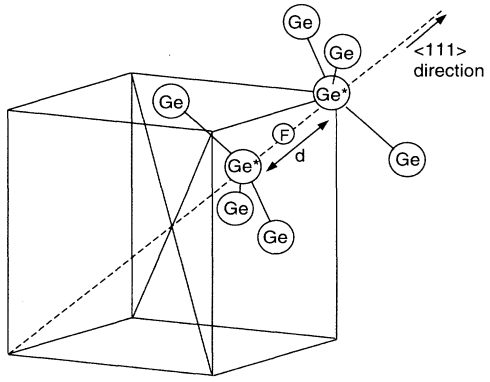

FIG. 4. The bond-centered cluster of FGe_8H_{18}. The ^{19}F atom is situated at the bond-centered site of Ge*-Ge* atoms in the ⟨111⟩ direction. Only heavy atoms are shown in the figure.

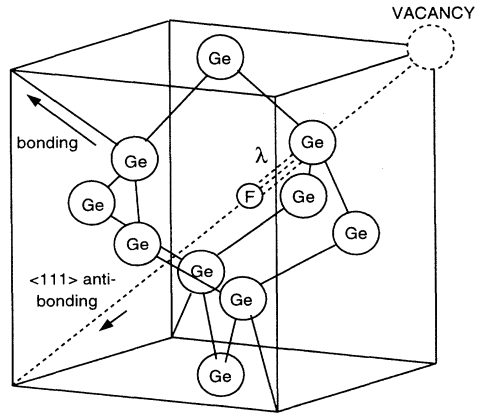

FIG. 5. The antibonding cluster of $FGe_{10}H_{15}$. The ^{19}F atom is situated along the ⟨111⟩ antibonding direction at a distance λ=1.8796 Å from a Ge atom. Only heavy atoms are shown in the figure.

TABLE II. Results of unrestricted Hartree-Fock (UHF), restricted Hartree-Fock (RHF), and density functional theory (DFT) calculations using STO-3G* basis functions at bond-centered (Fig. 4) and antibonding (Fig. 5) sites in Ge. For all cases η=0. The charge q_F on the fluorine atom obtained from the Mulliken process is given in units of e.

Site	Cluster	Method	q_F	V_{zz} (10^{22} V/m^2)
Bond-centered	FGe_8H_{18}	UHF	− 0.114	− 2.832
		DFT	+ 0.019	− 2.638
Antibonding	$FGe_{10}H_{15}$	RHF	− 0.204	− 2.650
		DFT	+ 0.010	− 1.996
		UHF	− 0.204	− 2.727
	This experiment :	ν_{Q1} = 27.5(3) MHz;		$\|V_{zz}\|$ = 1.58(9)
		ν_{Q2} = 33.0(4) MHz;		$\|V_{zz}\|$ = 1.90(11)

silicon with higher level basis sets,[21] it is therefore tempting to ascribe the 33.0-MHz and 27.5-MHz interactions to the bond-centered and antibonding sites, respectively. However, it is clear that more refined calculations are needed before such a conclusion can be definite.

In a comprehensive treatment of HF theory, Sahoo *et al.*[23] have considered such ⟨111⟩ sites in Ge for muonium at vacancy-associated and bond-centered locations. Similar impurity sites for fluorine have been postulated in silicon,[22–24] as well as for other impurities such as hydrogen,[25] deuterium,[26] and boron.[27]

B. Implantation of ^{19}F in GaAs

Figure 2, which shows the $R(t)$ spectrum obtained for ^{19}F implantation in GaAs, indicates a small quadrupole signal superimposed upon an exponential background, the latter possibly a result of randomly fluctuating time-dependent interactions.[13] The single quadrupole interaction, evident in the Fourier power transform of Fig. 3(b), is better featured in Fig. 3(a), where the exponential signal has been subtracted. The quadrupole interaction frequency was found to be axially symmetric (η=0) with ν_Q=27.7(5) MHz, corresponding to $|V_{zz}|$=1.59(9)×10^{22} V/m^2.

Since ^{19}F situated at antibonding sites with respect to Ga or As atoms would be expected to produce two distinct quadrupole interactions, we consider only the intrabond site (IB) shown in the $FGa_4As_4H_{18}$ cluster of Fig. 7, where dangling bonds have been saturated with H atoms. In this case the lowest energy of the system was obtained when the Ga-As bond length was increased from its lattice value of 2.4465 Å to 2.7713 Å, with the fluorine slightly displaced towards the Ga atom (x=1.3656 Å in Fig. 7).

The results of the calculations and corresponding Mulliken charge q_F are shown in Table III. They indicate a marked difference in the predictions of the HF and DFT methods, with the latter showing closer agreement with experiment. The DFT calculation, yielding V_{zz} =

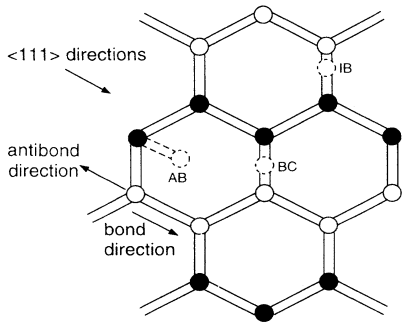

FIG. 6. Schematic representation of the sites in the {110} plane of the diamond lattice structure. Letters AB, BC, and IB indicate the antibonding, bond-centered, and intrabond sites, respectively.

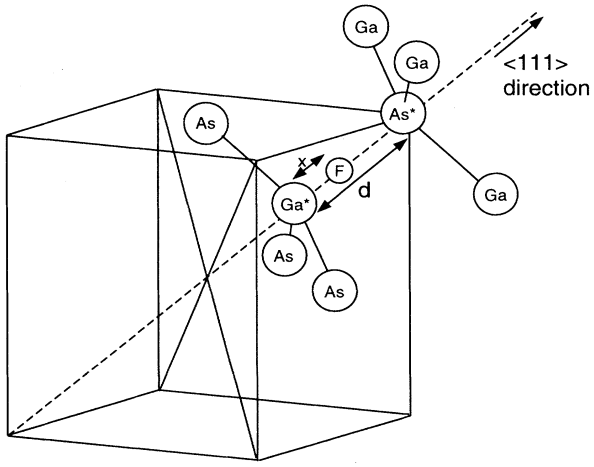

FIG. 7. The intrabond site in the cluster $FGa_4As_4H_{18}$. The ^{19}F atom is slightly displaced towards the Ga atom. The distances of Ga*-F and F-As* are 1.3656 and 1.4057 Å, respectively.

TABLE III. Results of restricted open-shell Hartree-Fock (ROHF) and density functional theory (DFT) calculations using STO-3G* basis functions at an intrabond site in the cluster $FGa_4As_4H_{18}$ (Fig. 7 with d=2.771 Å and x=1.366 Å). The charge q_F on the fluorine atom obtained from the Mulliken process is given in units of e.

Method	q_F	V_{zz} (10^{22} V/m^2)	η
ROHF	− 0.236	− 4.449	0
DFT	− 0.019	− 1.612	0
This experiment:		$\lvert V_{zz}\rvert$ = 1.59(9) ν_Q = 27.7(5) MHz	0.00(7)

-1.61×10^{22} V/m^2, or ν_Q=28.0 MHz, and η=0, compares favorably with the measured values of ν_Q=27.7(5) MHz and η=0.00(7).

In measurements involving TDPAD, the question of radiation damage must be addressed. It is known that the excited recoil nuclei typically slow down in less than 10^{-13} s in a sphere with a high defect concentration, and that local annealing can occur within 1 ns or less by migration and recombination.[28] Because of the high sensitivity of the measurements to the presence of local defects, radiation damage should be observable as a broadening in the quadrupole signal. In our measurements signal widths were typically less than 5%, which would appear to indicate minimal damage at the probe sites.

Dynamical considerations of the $^{19}F(p,p')^{19}F^*$ reaction support this contention. For the $p-^{19}F$ system the Coulomb barrier is 2.94 MeV, with closest distance of approach for a 2 MeV-proton of about 6.47 fm, more than twice the nuclear radius (3.2 fm) of ^{19}F. Moreover, when angular momentum transfer in the reaction is considered, an l=2 partial plane wave, for example, implies a classical impact parameter of about 7.8 fm. Consequently, Coulomb excitation is expected to play an important role, and at such high impact parameters, the scattered protons impart small recoil energies of a few keV or less to the recoiling $^{19}F^*$ nuclei. At such low recoil energies, radiation damage at probe sites would be expected to be small, and well removed from sites of maximum damage produced by the incident proton beam or from elastic recoils of ^{19}F nuclei.

VI. CONCLUSIONS

TDPAD measurements of quadrupole interactions involving the 197-keV isomeric state of ^{19}F confirm the presence of two quadrupole frequencies in Ge and indicate only a single frequency in GaAs. The axial symmetry of the interactions points to possible residence sites for F along ⟨111⟩ bonding and antibonding directions.

In the case of GaAs, DFT calculations at an intrabond site give ν_Q=28.0 MHz and η=0, in good agreement with the measured efg corresponding to an axially symmetric interaction with quadrupole frequency ν_Q=27.7(5) MHz. From energy considerations the F atom is predicted to be at distances of 1.37 and 1.41 Å from the Ga and As atoms, respectively.

For the Ge host poorer agreement with theory is obtained. The DFT calculations, however, yield efg values closer to experiment than the HF results. Based on the strong similarity with F sites in Si, and on the systematic trend of both DFT and HF predictions, it is suggested that the frequencies ν_{Q1}=27.5(3) MHz and ν_{Q2}=33.0(4) MHz correspond to F at an antibonding site 1.88 Å from a Ge atom and to a bond-centered site, respectively. More calculations with higher level basis sets are required, however, before a definite assignment can be made. With the rapid expansion in computing power and the ability to achieve complete hybridization of all electronic orbitals, the feasibility of realistic efg calculations in many electron system looks highly promising.

ACKNOWLEDGMENTS

Useful discussions with Dr. J. W. Bichard are greatly appreciated. To P. Rietveld we express our thanks for performing the sample evaporations. We are also extremely grateful for the support and assistance of Van de Graaff head Dr. A. Crametz and accelerator operators P. Falque, J. Leonard, and W. Schubert. One of us (P.W.M.) is indebted to IRMM for support throughout an enjoyable sabbatical visit. Another (D.S.) is grateful for support provided by the Government of Indonesia and for the hospitality of IRMM.

*Permanent address: Department of Physics, The University of British Columbia, 6224 Agricultural Road, Vancouver, British Columbia, Canada V6T 1Z1.

[1]Proceedings of Symposium F of the European Materials Research Society, Nuclear Methods in Semiconductor Physics, Strasbourg [Nucl. Instrum. Methods Phys. Res. Sect. B **63**, 1 (1992)].

[2]Y. Byoung-gon, N. Konuma, and E. Arai, J. Appl. Phys. **70**, 2408 (1991).

[3]Y. Nishioka, K. Ohyu, Y. Ohji, N. Natsuaki, K. Mukai, and T. P. Ma, IEEE Electron Device Lett. **EDL-10**, 141 (1989).

[4]P. J. Wright and K. C. Saraswat, IEEE Trans. Electron Devices **ED-36**, 879 (1989).

[5]Y. Nishioka, K. Ohyu, Y. Ohji, N. Natsuaki, and T. P. Ma, J. Appl. Phys. **66**, 3909 (1989).

[6]P. J. Wright, N. Kasai, S. Inoue, and K. C. Saraswat, IEEE Electron Device Lett. **EDL-10**, 347 (1989).

[7]Y. Nishioka, K. Ohyu, Y. Ohji., M. Kato, E. F. da Silva, Jr., and T.P. Ma, IEEE Trans. Nucl. Sci. **NS-36**, 2116 (1989).

[8]K. P. MacWilliams, L. F. Halle, and T. C. Zietlow, IEEE Electron Device Lett. **EDL-11**, 3 (1990).

[9]K. Ohyu, T. Itoga, Y. Nishioka, and N. Natsuaki, Jpn. J. Appl. Phys. **28**, 1041 (1989).

[10]B. Yu, N. Konuma, and E. Arai, J. Appl. Phys. **70**, 2408

(1991).
[11]K. Bonde Nielsen, T. Lauritsen, G. Weyer, H. K. Schou, and P. T. Nielsen, in Proceedings of the 6th International Conference on Hyperfine Interactions, Groningen, 1983 [Hyperfine Interact. **15/16**, 491 (1983)].
[12]P. W. Martin, D. Surono, F -J. Hambsch, H. Postma, and P. Rietveld, Hyperfine Interact. **77**, 315 (1993).
[13]T. Butz, Hyperfine Interact. **52**, 189 (1989).
[14]P. W. Martin, J. W. Bichard, and C. Budtz-Jørgensen, J. Chem. Phys. **93**, 6092 (1990).
[15]S. Connell, K. Bharuth-Ram, H. Appel, J. P. F. Sellschop, and M. Stemmet, Hyperfine Interact. **36**, 185 (1987).
[16]M. J. Frisch, G. W. Trucks, M. Head-Gordon, P. M. W. Gill, M. W. Wong, J. B. Foresman, B. G. Johnson, H. B. Schlegel, M. A. Robb, E. S. Replogle, R. Gomperts, J. L. Andres, K. Raghavachari, J. S. Binkley, C. Gonzales, R. L. Martin, D. J. Fox, D. J. Defrees, J. Baker, J. J. P. Stewart, and J. A. Pople, *Gaussian 92, Revision C* (Gaussian Inc., Pittsburgh, PA, 1992).
[17]J. Sauer, Chem. Rev. **89**, 199 (1989).
[18]A. D. Becke, J. Chem. Phys. **98**, 5648 (1993).
[19]C. Lee, W. Yang, and R. G. Parr, Phys. Rev. B **37**, 785 (1988).
[20]K. C. Mishra, K. J. Duff, and T. P. Das, Phys. Rev. B **25**, 3389 (1982).
[21]D. Surono, F-J. Hambsch, and P. W. Martin, Hyperfine Interact. **96**, 23 (1995).
[22]S. B. Sulaiman, N. Sahoo, K. C. Mishra, T. P. Das, and K. Bonde Nielsen, in Proceedings of the VIII International Conference on Hyperfine Interactions, Prague, 1989, edited by M. Finger, B. Sediak, and K. Zaweta [Hyperfine Interact. **60**, 861 (1990)].
[23]N. Sahoo, S. B. Sulaiman, K. C. Mishra, and T. P. Das, Phys. Rev. B **39**, 13 389 (1989).
[24]W. S. Verwoerd, Nucl. Instrum. Methods B **35**, 509 (1988).
[25]V. A. Singh, C. Weigel, J. W. Corbett, and L. M. Roth, Phys. Status Solidi **81**, 637 (1977).
[26]S. T. Picraux and F. L. Vook, Phys. Rev. B **18**, 2066 (1978).
[27]G. D. Watkins, Phys. Rev. B **12**, 5824 (1975).
[28]W. Kreische, H. -U. Maar, H. Niedric, K. Reuter, and K. Roth, Hyperfine Interact. **4**, 732 (1978).